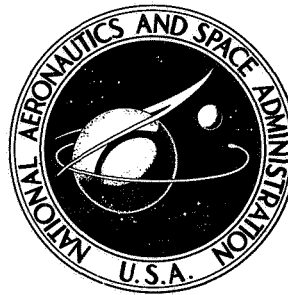


NASA TECHNICAL NOTE



NASA TN D-7636

NASA TN D-7636

**CASE FILE
COPY**

**EFFECT OF GEOMETRICAL
AND FLOW PARAMETERS ON
HIGH-EFFECTIVENESS REGION
OF FILM COOLING**

by Willis H. Braun

Lewis Research Center

Cleveland, Ohio 44135



NATIONAL AERONAUTICS AND SPACE ADMINISTRATION • WASHINGTON, D. C. • APRIL 1974

1. Report No. NASA TN D-7636	2. Government Accession No.	3. Recipient's Catalog No.	
4. Title and Subtitle EFFECT OF GEOMETRICAL AND FLOW PARAMETERS ON HIGH-EFFECTIVENESS REGION OF FILM COOLING		5. Report Date APRIL 1974	6. Performing Organization Code
		8. Performing Organization Report No. E-7538	
7. Author(s) Willis H. Braun		10. Work Unit No. 502-04	11. Contract or Grant No.
9. Performing Organization Name and Address Lewis Research Center National Aeronautics and Space Administration. Cleveland, Ohio 44135		13. Type of Report and Period Covered Technical Note	
		14. Sponsoring Agency Code	
12. Sponsoring Agency Name and Address National Aeronautics and Space Administration Washington, D.C. 20546		15. Supplementary Notes	
16. Abstract <p>Previous analyses for an inviscid jet injected into a stream and the turbulent mixing region which forms between jet and stream are used to find the extent of the core region in a cooling film by calculating the growth of the turbulent boundary layer on the downstream wall. The core is a region of nearly perfect effectiveness which ends at the intersection of the boundary layer and the mixing region. The calculations show that the most important geometrical factor bearing on the length of the core is the curvature of the wall. When the radius of curvature is large, the boundary layer remains thin and the core is long. The effects of Reynolds number, total-pressure difference between film and stream, and lateral position of the downstream wall are also investigated. The step configuration is shown to have a longer core than the slot for the same flow conditions.</p>			
17. Key Words (Suggested by Author(s)) Film cooling; Jet mixing; Wall jet; Jet injection; Jet core		18. Distribution Statement Unclassified - unlimited Category 33 Cat. 33	
19. Security Classif. (of this report) Unclassified	20. Security Classif. (of this page) Unclassified	21. No. of Pages 30	22. Price* \$3.25

* For sale by the National Technical Information Service, Springfield, Virginia 22151

EFFECT OF GEOMETRICAL AND FLOW PARAMETERS ON HIGH-EFFECTIVENESS REGION OF FILM COOLING

by Willis H. Braun
Lewis Research Center

SUMMARY

Previous analyses for an inviscid jet injected into a stream and the turbulent mixing region which forms between jet and stream are used to find the extent of the core region in a cooling film by calculating the growth of the turbulent boundary layer on the downstream wall. The core is a region of nearly perfect effectiveness which ends at the intersection of the boundary layer and the mixing region. The calculations show that the most important geometrical factor bearing on the length of the core is the curvature of the wall. When the radius of curvature is large, the boundary layer remains thin and the core is long. The effects of Reynolds number, total-pressure difference between film and stream, and the lateral position of the downstream wall are also investigated. The step configuration is shown to have a longer core than the slot for the same flow conditions.

INTRODUCTION

A wide variety of geometrical designs has been used in the experimental study of film cooling, all of them having the purpose of providing an insulating layer of fluid along a wall to protect it from the temperature or chemical composition of an external, flowing stream. (A comprehensive catalog of the devices is given by Goldstein (ref. 1).) The development of such a film and its interaction with the main stream may usually be divided into three regions, as pointed out by Seban and Back (ref. 2) and also by Stollery and El-Ehwany (ref. 3). Immediately after injection, there may be a potential core region similar to that found in a free jet. The core is diminished by the mixing of the film with the external stream and by the growth of a boundary layer on the downstream wall. When the mixing zone and the boundary layer merge to terminate the core, a wall-jet region is formed in which the mean-velocity profile may have a vanishing slope at more than one point. Finally, the velocity profile smooths out, and a boundary-layer region completes the flow.

Each of the regions has been the subject of analysis. Hatch and Papell (ref. 4) employed a model which treated the coolant film as a discrete layer, unmixed with the external stream, and derived a correlation which fit their experimental data well for as much as 100 slot heights downstream of the coolant entrance. An analysis by Pai and Whitelaw (ref. 5) ignores the core region and treats the film as a wall jet immediately after injection. Under this condition the heat transfer and the effectiveness of the film are obtained taking into account slot-lip thickness, velocity ratio, density ratio, and longitudinal pressure gradient. Analyses which have used mainly a boundary-layer model of film cooling are those of Seban and Back (ref. 6), Stollery and El-Ehwany (ref. 3), and Nicoll and Whitelaw (ref. 7). Each of these analyses predicts the effectiveness of film cooling in the boundary-layer region.

In this report, attention is given to the injection region where the film fluid and the external fluid first meet. Both the internal geometry of the slot and the conditions which the film meets when it encounters the stream have a significant effect upon the length of the core. Provided there is not significant molecular transport across the core, its length defines the distance over which the wall is nearly perfectly insulated from the stream. This report attempts to show the effect of reservoir wall shape, wall position, Reynolds number, and total-pressure difference on the extent of the core.

DESCRIPTION OF FLOW ANALYSES

Regions of Potential and Turbulent Flow

The basis of the analysis to be presented herein is the description of an attached inviscid jet given by Goldstein and Braun (ref. 8). As pictured therein the jet flows from a reservoir, through an orifice between two semi-infinite walls, and into a stream, as shown in figure 1. The difference in total pressure between jet and stream is assumed to be small. The growth of the viscous mixing region along the slip line between the outer stream and the jet was analyzed by Braun and Goldstein (ref. 9). In these studies the walls were considered to be infinitesimally thin. This assumption is especially critical for the fluid traveling the streamline adjacent to the downstream wall. As the fluid leaves the reservoir along the underneath surface of the wall, it travels toward the lip at increasing speed. The velocity which it reaches as it rounds the lip is unbounded, and the adverse pressure gradient through which it must flow as it moves along the upper surface is very strong. This description of the motion is valid for a perfect fluid. But when such conditions are imposed on a real viscous fluid, the boundary layer on the wall cannot negotiate the pressure gradient, and separation occurs at the lip.

To avoid this situation, and to approximate more closely a real configuration, the downstream wall is represented herein by a streamline of the inviscid jet, as shown in

figure 2. Since the inviscid-flow solution provides the pressure gradient along the streamline, the development of a boundary layer on the corresponding wall may be studied. Inasmuch as the fluid starts from rest before issuing from the reservoir, it is assumed that the core remains a potential flow and continues to act as an insulator until the boundary layer and the mixing region meet. At that point the wall and stream are connected by a turbulent diffusion process.

The parameters which govern the injection process are both geometrical and fluid related. One parameter chosen to characterize the downstream wall is the angle σ (fig. 2), far in the reservoir, which the wall makes with the positive horizontal direction. An additional degree of freedom arises from the choice of the orifice angle α (figs. 1 and 2) of the inviscid flow, which is a second geometrical parameter. The Reynolds number of the film and the difference of total pressure between film and stream introduce the properties of the fluid and the flow conditions. If the total pressure film and stream are equal, there will be no velocity difference between them where they join - and no mixing. Therefore, it can be anticipated that film cooling will be most effective for velocity ratios near 1, as has, indeed, been demonstrated experimentally by Samuel and Joubert (ref. 10) and Kacker and Whitelaw (ref. 11). For this reason the restriction of the basic inviscid flow to small total-pressure differences is not a severe limitation on the model.

Two types of common injection geometry are modeled herein. If the downstream wall lies in a plane displaced below the plane of the upstream wall, the configuration is referred to as a backward-facing step or, simply, a "step." On the other hand, in the "slot" arrangement the jet emerges from an opening between upstream and downstream walls which lie in the same plane. Both of these geometries can be approximated by making suitable choices of orifice angle and streamline in the theoretical inviscid flow, as shown in figures 3 and 4. In contrast to the more general configurations treated in references 8 and 9, the downstream wall in the cases treated herein is never higher than the upstream wall.

Several other limitations in the scope of the treatment are made. It is assumed that the fluids of film and stream are incompressible and of the same density. The mixing region is assumed to be turbulent, and the boundary layer is assumed to undergo transition from laminar to turbulent flow at the station on the downstream wall where the velocity outside the boundary layer reaches a maximum. This maximum occurs near the point of maximum curvature on the wall and is midway in the motion of a fluid particle between its acceleration from rest in the reservoir and its deceleration to a velocity near that of the free stream. If the wall is smooth, experience with boundary layers on airfoils indicates that transition will not occur ahead of the velocity maximum (ref. 12).

Basic Inviscid Flow

The inviscid flow described by Goldstein and Braun (ref. 8) is illustrated in figure 1. An orifice is formed by two semi-infinite, parallel walls which are not, in general, coplanar. The jet issues from the reservoir below the orifice and displaces the stream upwards as it flows along the downstream wall. The streamline common to stream and jet is the slip line, across which there is generally a jump in velocity. The magnitude of the velocity jump is proportional to the parameter

$$\epsilon = \frac{P_j - P_\infty}{\frac{1}{2} \rho V_\infty^2} \quad (1)$$

where P_j and P_∞ are the total pressures of the jet and stream, respectively. (Symbols are defined in appendix A.) The theory is restricted to small ϵ so that the flow quantities may be expressed as a power series in ϵ . The complete details of the development are given by Goldstein and Braun (ref. 8). It is only necessary here to repeat some of the results which provide the velocity field and streamlines of the flow.

The zeroth-order terms in the ϵ expansions for the complex conjugate velocity $u - iv$ and the complex potential $\varphi + i\psi$ are related to position by parametric relations

$$u - iv = \frac{U - iV}{V_\infty} = \frac{T}{T - \Delta} \quad (2)$$

$$\varphi + i\psi = \frac{\Phi + i\Psi}{V_\infty H_0} = \frac{1}{\pi} (T + 1 + \ln T) - i \quad (3)$$

$$x + iy = \frac{X + iY}{H_0} = \frac{1}{\pi} \left[T + (1 - \Delta) \ln T + \frac{\Delta}{T} + 1 + \Delta \right] + (\Delta - 1)i \quad (4)$$

The intermediate variable $T \equiv \xi + i\eta$ ($\eta \geq 0$) which appears on the right side of these equations is the variable of an auxiliary mapping plane used in the solution of the flow problem, and Δ is a parameter related to the angle α which the orifice opening makes with the horizontal:

$$\alpha = \tan^{-1} \frac{\pi (\Delta - 1)}{(1 - \Delta) \ln \Delta + 2(1 + \Delta)} \quad (5)$$

The characteristic length H_0 is the asymptotic width of the jet, to order zero in ϵ , as it moves downstream. Since, also to order zero, the jet velocity approaches the stream velocity V_∞ , the dimensionless stream function ψ has a span of unity across the jet.

The slip line is labeled $\psi = 0$ and the downstream wall $\psi = -1$.

Along a specific streamline in the jet, equation (3) yields

$$\pi\psi = \eta + \tan^{-1} \frac{\eta}{\xi} - \pi \quad (6)$$

from which

$$T = \frac{\eta e^{i(\sigma-\eta)}}{\sin(\sigma-\eta)} \quad (7)$$

where

$$\sigma = \pi(1 + \psi) \quad -1 \leq \psi \leq 0 \quad (8)$$

If the streamline specified in equation (6) is used to represent a wall, then σ , given by equation (8), is the angle which the wall makes with the horizontal far back in the reservoir, as illustrated in figure 2.

Film-Cooling Configurations

Step. - The jet flow described by equations (1) to (8) can be used to represent the geometry of various film-cooling configurations by selecting appropriate values of stream function ψ and the parameter Δ . Consider first the backward-facing "step," in which the downstream wall is parallel to but situated below the upstream wall.

If x_w, y_w denote dimensionless wall coordinates, equation (4) on the streamline (eq. (7)) yields

$$x_w = \frac{1}{\pi} \left[\eta \cot(\sigma - \eta) + (1 - \Delta) \ln \frac{\eta}{\sin(\sigma - \eta)} + \frac{\Delta \sin 2(\sigma - \eta)}{2\eta} + 1 + \Delta \right] \quad (9)$$

$$y_w = \frac{1}{\pi} \left[\eta + (1 - \Delta)(\sigma - \eta) - \frac{\Delta \sin^2(\sigma - \eta)}{\eta} \right] + \Delta - 1 \quad (10)$$

for its real and imaginary parts, respectively.

A family of four steps, defined by equations (9) and (10), is illustrated in figure 3, with the wall of the corresponding inviscid flow shown as a dashed line. The family was constructed by choosing four streamlines in an inviscid flow for which the orifice angle was $\alpha = -\pi/2$. The four values of stream function, $\psi = -0.2, -0.4, -0.6,$ and -0.8 , are related to the wall angles by equation (8). The value of Δ corresponding to the specified value of α is obtained by observing that for $\alpha = -\pi/2$ equation (5) requires

$$(1 - \Delta) \ln \Delta + 2(1 + \Delta) = 0$$

or

$$\Delta = 0.0908 \quad (11)$$

It can be seen from equation (9) that the condition $x \rightarrow \infty$ is obtained by letting $\eta \rightarrow \sigma$. If this limit is inserted in equation (10), the asymptotic wall level is given by

$$\lim_{\eta \rightarrow \sigma} y_w = \frac{\sigma}{\pi} + \Delta - 1 = \Delta + \psi \quad (12)$$

Since the upstream wall is located in the plane $y = 0$, the dimensionless height of the step, that is, the asymptotic vertical displacement between the walls, is obtained in units of H_0 from equation (12) as

$$S = 0 - \lim_{\eta \rightarrow \sigma} y_w = (\psi + \Delta) \quad -1 \leq \psi \leq 0 \quad (13)$$

Slot. - As a second type of configuration, figure 4 shows a family of horizontal "slots" which meet the condition that the streamline representing the downstream wall is (asymptotically) coplanar with the upstream wall. The relation between ψ and Δ that is imposed can be found by setting the asymptotic y_w found from equation (12) equal to zero far downstream. Thus, the condition for a slot is

$$\Delta = -\psi \quad (14)$$

Since condition (14) specifies one streamline for each orifice angle α (or Δ), the curves of figure 4 are streamlines from different flows so that it is permissible for them to cross.

Mixing Region

The mixing region (fig. 2) between the jet and the stream has been treated by Braun and Goldstein (ref. 9) for both turbulent and laminar mixing. When flows of different velocities join at the lip of the upstream wall, the action of viscosity smooths out the velocity discontinuity. A mixing region with a continuous velocity profile begins to diffuse outward from the inviscid slip line. It is assumed in the cases studied herein that the mixing region is entirely turbulent. Then the velocity profile in the mixing region is given by

$$u = V_s^+ - \epsilon \frac{V_\infty^2}{4V_{s,0}} \left[1 + \operatorname{erf} \left(\frac{N}{2\sqrt{s_t}} \right) \right] \quad (15)$$

where N is a dimensionless coordinate normal to the slip line and s_t is a longitudinal coordinate of dimension length-squared and measured from the lip as described in reference 9. The coordinate s_t is related to the running variable η along the slip line by

$$\frac{s_t}{H_0^2} = \frac{\kappa|\epsilon|}{2} \int_0^\eta \left[\frac{V_\infty}{V_{s,0}(\gamma)} \right]^3 \frac{\hat{S}_0(\gamma)}{H_0} J(\gamma) d\gamma \quad (16)$$

Here

$$\frac{\hat{S}_0}{H_0} = \int_0^\eta \frac{V_\infty}{V_{s,0}(\gamma)} J(\gamma) d\gamma \quad (17)$$

and the Jacobian is

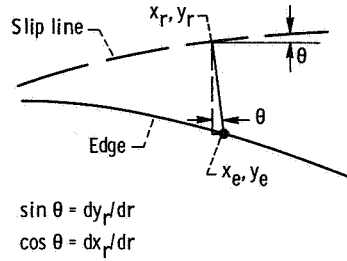
$$J(\gamma) = \frac{(1 - \gamma \cot \gamma)^2 + \gamma^2}{\pi\gamma} \quad (18)$$

and κ is an empirical coefficient which has a value of about 0.002. The value given to κ depends upon the conditions upstream of the lip at which the stream and jet join. In the experiments of Mills (ref. 13), from which the value used herein was obtained, the boundary layers on the top and bottom sides of the upstream wall were symmetric and accelerating. This corresponds to the condition of the lower boundary layer in the issuing jet studied herein, but not necessarily to the upper boundary layer.

If the thickness of the mixing region $2\delta_t$ is defined by choosing for the half-width the distance from the slip line at which 0.99 times the velocity difference between stream and jet is reached, then

$$\delta_t = 3.29 \sqrt{s_t} \quad (19)$$

The coordinates of the edge of the mixing region may be constructed by marking off perpendicular to the slip line a length equal to the half-thickness at that distance from the upstream lip. This operation relates the point of the edge (x_e, y_e) to its corresponding point on the slip line (x_r, y_r) by (see sketch)



$$\left. \begin{aligned} x_e &= x_r + \delta_t \frac{dy_r}{dr} \\ y_e &= y_r - \delta_t \frac{dx_r}{dr} \end{aligned} \right\} \quad (20)$$

where dr is an element of arc along the slip line. The coordinates (x_r, y_r) of the slip line are given by the real and imaginary parts, respectively, of equation (4) with T represented by equation (7) and $\sigma = \pi$.

Boundary Layer

The fluid in the reservoir starts nearly at rest, according to the model used herein, and accelerates on its way to the exit. The boundary layer on the walls becomes thinner, therefore, in the direction of fluid motion. Boundary layers of this type have been labeled "backwards" boundary layers (ref. 14). Examples of the distribution of momentum thickness, displacement thickness, and skin friction in laminar backwards boundary layers are given by Ackerberg and Glatt (ref. 15).

It is assumed herein that the backwards boundary layer which forms on the downstream wall is laminar in the reservoir and that transition to turbulence occurs at the point along the wall where the velocity of the inviscid flow reaches a maximum. The terminal value of momentum thickness of the laminar boundary thus provides the initial condition for the turbulent boundary layer. Although no practical reservoir will be of infinite extent, the examples given by Ackerberg and Glatt yield estimates of the terminal momentum thickness which should be satisfactory. A typical value is

$$\frac{\theta}{L} = \frac{0.04}{\sqrt{Re}} \quad (21)$$

Here L is a characteristic length for the flow, set equal to the step height H_0S for the

step configuration and equal to the minimum distance $H_0 d$ across the opening in the case of the slot:

$$d = \left(\sqrt{x^2 + y^2} \right)_{\min} \quad (22)$$

The value of the momentum thickness given by equation (21) is used as an initial condition for each of the turbulent boundary layers treated herein. Calculations using four times the constant given in equation (21) show that the boundary-layer development is not sensitive to the value used.

The method chosen to follow the development of the boundary layer after transition is the integral method of Garner (ref. 12), which is especially adapted to turbulent boundary layers in adverse pressure gradients. The momentum equation takes the form

$$\frac{d\Theta}{ds} = \frac{n+1}{n} \left[\zeta - \frac{\Theta}{W} \frac{dW}{ds} \left(H + \frac{2n+1}{n+1} \right) \right] \quad (23)$$

where the dependent variable Θ is related to the momentum thickness by

$$\Theta = \theta R_\theta^{1/n} \quad (24)$$

and the independent variable s is the arc length measured along the surface. The parameters ζ and n were found empirically to have the values

$$\left. \begin{array}{l} \zeta = 0.006534 \\ n = 6 \end{array} \right\} \quad (25)$$

An auxiliary equation for the form factor H is

$$\Theta \frac{dH}{ds} = e^{5(H-1.4)} \left[- \frac{\Theta}{W} \frac{dW}{ds} - 0.0135 (H - 1.4) \right] \quad (26)$$

The magnitude W of the velocity outside the boundary layer, which appears in the right side of this equation as well as in the momentum equation, is obtained from equation (2) as

$$W = \sqrt{u^2 + v^2} V_\infty = \sqrt{\frac{T\bar{T}}{(T - \Delta)(\bar{T} - \Delta)}} V_\infty \quad (27)$$

with T given by equation (7). The differential arc length is obtained from

$$ds = \sqrt{d(x+iy) d(x-iy)} H_0 \quad (28)$$

by using equation (4) and (7). In addition to the condition that θ be continuous, the system of equations (23) and (26) has the initial condition on H that $dH/ds = 0$. According to Garner, if transition occurs at the velocity maximum, the condition on H is equivalent to setting $H = 1.4$ immediately after transition.

One caution must be exercised with this method of boundary-layer solution. The momentum equation (23) is valid only under the restriction

$$0 < -\frac{\Theta}{W} \frac{dW}{ds} < 0.01 \quad (29)$$

This restriction is met in all the calculations made herein.

To find the locus of the boundary-layer edge, it is necessary to know the actual thickness rather than the momentum thickness. If it is assumed that a 1/7-power velocity profile is an adequate description of the real profile, the boundary-layer thickness is given by

$$\delta = \frac{72}{7} \theta \quad (30)$$

The location of a point (x_δ, y_δ) on the edge of the boundary layer corresponding to a point (x_w, y_w) on the wall is given by

$$\left. \begin{aligned} x_\delta &= x_w - \delta \frac{dy_w}{ds} = x_w - \delta \frac{dy_w/d\eta}{ds/d\eta} \\ y_\delta &= y_w + \delta \frac{dx_w}{ds} = y_w + \delta \frac{dx_w/d\eta}{ds/d\eta} \end{aligned} \right\} \quad (31)$$

Core Length

The foregoing descriptions of the two viscous flow regimes, the mixing region and the boundary layer, have been used to find the extent of the core region for several steps and slots constructed from the basic inviscid flow. By finding graphically the intersection of the edge of the mixing zone as expressed in equation (20) with the edge of the boundary layer as given by equation (31), an estimate of the core length x_1 (fig. 2) has been found for several Reynolds numbers and total-pressure differences. Reynolds numbers of 10 000, 100 000, and infinity, based on characteristic lengths $H_0 S$ or $H_0 d$ as appropriate, have been used. The first two values are typical of experimental film-cooling flows. The third yields a limit for very thin boundary layers for which the mixing zone reaches to the wall.

For the step configuration, several values of orifice angle α near $-\pi/2$ were used to study the effect of a small range of this variable. The values of orifice angle corresponding to values of the parameter Δ are given in the following table:

Δ	α , deg
0.05	-104.0
.07	-96.5
.09	-90.2
.11	-84.8
.13	-79.9

The range of dimensionless pressure difference ϵ was determined by estimating the coefficients of the first power of ϵ in the expansions of velocity and streamline position in the jet. The calculations made in appendix B show that if $|\epsilon| < 0.2$, the description of the inviscid flow in which the boundary layer grows will be in error by about 10 percent if only the zero-order terms are employed. If 10 percent is also taken as an estimate of the effect of velocity and stream-function errors on the position of the boundary-layer edge, using only zero-order calculations of the inviscid flow appears to be justified.

The estimate of the position of the mixing-region edge comes from the first-order term in the expression for the velocity profile (eq. (15)). If the second-order term in ϵ has a coefficient which is of order 1, the error from an $|\epsilon| < 0.2$ should be negligible. The most likely source of error in the mixing-region computation is the choice of the numerical coefficient κ which, although given the value 0.002 here, actually varies in experiment from 0.00139 to 0.00251. (The κ used herein corresponds to κC of Mills (ref. 13).) It is also assumed herein that the upstream wall is thin compared to the step height or slot width so that there is no separation of the flow. Separation has been shown by Burns and Stollery (ref. 16) and Kacker and Whitelaw (ref. 17) to have serious adverse effects on film-cooling efficiency.

RESULTS AND DISCUSSION

Step Film-Cooling Configuration

The curves of figures 5 to 7 show the effects of varying wall angle, orifice angle of the basic inviscid flow, dimensionless total-pressure difference, and Reynolds number based on step height,

The desirability of a very gentle curvature of the downstream wall (large σ) is

immediately apparent in all the curves. The longer core length which is always found at higher wall angles can be attributed to a thinner boundary layer, which itself is the result of a reduced adverse pressure gradient.

On the other hand, when the wall angle is reduced to the neighborhood of 35° to 40° , corresponding to a sharp bend in the wall, the strongly adverse pressure gradient separates the boundary layer and the core length begins to drop off rapidly. The lower ends of the curves represent angles at which the boundary layer is still unseparated before intersection with the four mixing layers characterized by $\epsilon = 0, 0.05, 0.10, \text{ and } 0.20$. The slightest decrease of wall angle from these values brings the point of separation sharply forward to the knee of the wall. It may be assumed that a separated boundary layer would intersect the mixing region at an earlier station along the wall than if it had remained attached. Since the separated boundary layer is not described by the analysis used herein, no attempt has been made to obtain the core length below wall angles leading to separation.

Although the curves rise steeply in the neighborhood of $\sigma = 150^\circ$, they should not be interpreted as rising without bound. The boundary layers always grow with distance down the wall and the core will, therefore, always be of finite extent. Moreover, the long cores in this region will be difficult to attain in practice because the analysis presupposes that the (narrow) reservoir is long enough for the fluid to be initially at rest.

If the orifice angle for the basic inviscid flow is adjusted so that the downstream wall as a unit is moved downstream (α less negative or Δ increasing), the core length is increased. This result can be attributed to two effects. The first effect is a reduction of the maximum velocity external to the boundary layer, because the mouth is wider, so that the magnitude of the adverse pressure gradient is reduced. The second effect is a simple shifting of the wall and its boundary layer downstream, which delays the intersection with the mixing layer.

Another parameter which affects the boundary layer is the Reynolds number. Inasmuch as a large Reynolds number leads to thin boundary layer, it is expected that the core length should increase with Reynolds number. This is borne out by calculations which show that Reynolds number has a moderate effect of this sort, leading to an increase of core length in the neighborhood of 25 percent in going from $Re_S = 10\,000$ to $Re_S = 100\,000$. The curves labeled $Re_S = \infty$ were obtained by assuming that the boundary layer has zero thickness so that the edge of the mixing region intercepts the wall. These curves represent an upper limit on core length for each of the three strengths of mixing zone $\epsilon = 0.05, 0.10, \text{ and } 0.20$. If the dimensionless pressure difference ϵ vanishes at the same time that the Reynolds number is infinite, there is neither a mixing zone nor a boundary layer. The film is then entirely inviscid at all distances from the reservoir mo-

Reynolds number, orifice angle, and wall angle affect mainly the boundary layer. In contrast, the difference in total pressure between film and stream determines the growth of the mixing region and, therefore, its intersection with the boundary layer at

the terminus of the core. Figures 5 to 7 show core length for four values of dimensionless pressure difference ϵ . An improvement by a factor of 2 in core length can be obtained by reducing ϵ from 0.20 to 0 at a Reynolds number of 10 000. Since the theory for the growth of the mixing region is symmetric in ϵ , a maximum of core growth is obtained for $\epsilon = 0$, that is when there is no velocity difference between film and stream. This result has been shown experimentally by Whitelaw (ref. 18).

In addition to knowing the dimensionless core length x_1/S for any set of values of σ , Δ , ϵ , and Re_S , it is desirable to examine the results while taking into account the amount of flow required to establish the film. The mass flow in the film is $V_\infty H_0 |\psi|$, where ψ is the value of the stream function on the wall. If the film length $H_0 x_1$ is multiplied by the characteristic velocity V_∞ and divided by the mass flow, the result is an efficiency index $x_1/|\psi|$ which adjusts the length of the core by the amount of fluid the film uses to provide the insulation. This quantity is displayed in figure 8 for the ranges of parameters previously used. Although the shapes of the curves are qualitatively the same as those for the core length x_1/s , the efficiency index does not rise as steeply with wall angle because at the higher wall angles relatively more fluid is being fed into the film. It is also apparent that separation occurs at much higher wall angles, around 86° to 88° for the Reynolds numbers investigated herein. This emphasizes the desirability of introducing the fluid in a streamwise direction through the slot.

Slot Film-Cooling Configuration

Figure 9 shows how the dimensionless core length of a film issuing from a slot varies with the three parameters σ , ϵ , and Re_d . Again, as with the step configuration, the advantage of having a gentle curve in the downstream wall is emphasized by the rise of the curves with increasing wall angle. The general level of the curves is not as high, however, indicating that the step configuration discharges a film with a longer core. It is also apparent that the improvement in core length with wall angle is less emphatic for the slot. Improvement of less than a factor of 2 is obtained with the slot film in going from the low end to the high end of the σ range. With the step film, by contrast, an order of magnitude change in core length can be obtained.

The adverse effect of a strong pressure gradient can be observed in the contrast of figures 9(a) and (b) with 9(c). When there is no boundary layer ($Re_d = \infty$), the core length increases as the wall angle drops to low values. If a boundary layer is present (figs. 9(a) and (b)), it thickens so severely that the core length actually drops.

An efficiency index can be constructed in the same way as for the slot and is shown in figure 10. As can be seen from figure 10(c), the efficiency index is nearly independent of wall angle when there is no boundary layer.

CONCLUDING REMARKS

An analysis was performed to determine the effect of geometrical and flow parameters on the extent of the core region in a cooling film. In interpreting the results of the analysis, it is important to remember the ways in which the basic inviscid flow provides favorable conditions which may not always be met in experimental apparatus. In the model the fluid starts from rest in the reservoir and it is, therefore, appropriate to assume that there is no residual turbulence in it. This condition would not correspond to an experiment in which the coolant is brought to the stream in a long channel of essentially constant width. Such a configuration is likely to generate a high level of turbulence.

In many practical applications, the turbulence and/or the gross pressure fluctuations in the main stream may make it impossible to maintain the desirable small values of ϵ . Consequently, in examining such a real case, data relating to the root-mean-square pressure fluctuations should be gathered before an effective value of ϵ is assigned.

The model used herein also insures a nearly tangential introduction of film even for the slot configuration. This model is in contrast to many experimental setups in which the coolant is turned sharply before the mouth. Such geometries are equivalent to using a low value of wall angle in the present model and most likely lead to separation of the flow and generation of turbulence.

The implicit assumption that the upstream lip is thin is satisfied by most experimental arrangements. Even when it does not hold, however, the effects of pressure difference, wall angle, orifice angle, and Reynolds number will remain qualitatively the same. A similar remark can be made about the effect of the boundary layer upstream. Even though it is not likely to be symmetric with the boundary layer on the reservoir side of the wall, it will not make a qualitative difference in the curves for film length.

Lewis Research Center,
National Aeronautics and Space Administration,
Cleveland, Ohio, December 20, 1973,
502-04.

APPENDIX A

SYMBOLS

d	slot width, eq. (22)
H	form factor of boundary layer
H_0	asymptotic width of inviscid jet to order zero in ϵ
h_1	dimensionless first-order correction to H_0
J	Jacobian
L	characteristic length, $H_0 S$ for step and $H_0 d$ for slot
N	normal coordinate in mixing zone
n	number defined by eq. (25)
P_j	total pressure of jet or film
P_∞	total pressure of stream
Re	Reynolds number, $V_\infty L/\nu$
Re_d	Reynolds number based on slot width
Re_S	Reynolds number based on step height
Re_θ	Reynolds number based on momentum thickness
r	distance along slip line
S	step height, eq. (13)
\hat{S}	distance along slip line
s	distance measured along downstream wall
s_t	derived longitudinal coordinate for mixing zone
T	complex variable in a mapping plane, $T = \xi + i\eta$
U, V	X- and Y-components of velocity
u, v	dimensionless velocity components, U/V_∞ and V/V_∞
V_S^+	velocity along slip line, inside of inviscid jet

V_s^-	velocity along slip line, in external stream
$V_{s,0}$	zeroth approximation to velocity along slip line
V_∞	free-stream velocity
W	velocity of fluid outside boundary layer
X, Y	Cartesian coordinates
x, y	$X/H_0, Y/H_0$
x_i	abscissa of intersection of boundary layer and mixing zone
α	orifice angle of inviscid jet, eq. (5)
Γ	function defined by eq. (B4)
γ	dummy variable to replace η
Δ	parameter related to orifice angle, eq. (5)
δ	boundary-layer thickness
δ_t	half-thickness of mixing layer
ϵ	dimensionless pressure difference, defined by eq. (1)
ζ	number defined by eq. (25)
η	imaginary part of T
Θ	modified momentum thickness
Θ^+	line integral defined by eq. (B3)
θ	momentum thickness of boundary layer
κ	empirical constant
ν	kinematic viscosity
ξ	real part of T
ρ	density of fluid
σ	wall angle defined by eq. (8)
τ	dummy variable
Φ, Ψ	potential and stream functions
φ, ψ	dimensionless potential and stream functions, $\Phi/V_\infty H_0$ and $\Psi/V_\infty H_0$

Subscripts:

e edge of mixing region

s slip line

w wall

δ edge of boundary layer

Superscript:

— overbar, complex conjugate

APPENDIX B

FIRST-ORDER CORRECTIONS

Consider, as an example of a first-order correction to the inviscid flow, the increment in asymptotic jet width caused by a difference in total pressure between jet and stream. The width to order ϵ is given by Goldstein and Braun (ref. 8) as

$$H = H_0 (1 + \epsilon h_1 + \dots) \quad (\text{B1})$$

They show further that

$$h_1 = \Theta^+(0) \quad (\text{B2})$$

where Θ^+ is a line integral along the slip line given as

$$\Theta^+(T) = \frac{1}{2\pi i} \int \frac{\Gamma(\tau) d\tau}{\tau - T} - \frac{1}{2\pi i} \int \frac{\overline{\Gamma(\tau)} d\overline{\tau}}{\overline{\tau} - T} \quad \text{Re } T \geq 0 \quad (\text{B3})$$

The function Γ appearing in the integrals is defined by

$$\Gamma = \frac{-i}{u - iv} \text{Im} \frac{1}{u - iv} \quad (\text{B4})$$

where it is understood that the velocity components u, v are the zero-order approximations as given by equation (2). When equation (7) for the streamline is introduced into equation (B4), the integration of equation (B3) can be performed at $T = 0$ with the result

$$h_1 = \frac{\text{Si}(2\pi)}{2\pi} \Delta(1 + \Delta) = 0.2257 \Delta(1 + \Delta) \quad (\text{B5})$$

In the step configuration, the parameter $\Delta \ll 1$, so that the change in inviscid jet width and, therefore, the displacement of streamlines is of order $\Delta\epsilon$. So for this case the displacement of streamlines is negligible even to first order in ϵ , and the characteristic length is unaffected. The same cannot be said for the velocity perturbations of first order, for Goldstein and Braun show that far out in the jet

$$u \rightarrow \sqrt{1 + \epsilon}$$

which is independent of Δ .

In the slot configuration, Δ is no longer small compared to 1 and becomes as large as 0.52, corresponding to a wall angle at which the boundary layer separates. However,

the displacement of streamlines of the jet, other than the outermost, is given by

$$\epsilon h_1 (1 + \psi) = \epsilon h_1 (1 - \Delta) = 0.2257 \epsilon \Delta (1 - \Delta^2)$$

The change in the characteristic length L is, then,

$$\Delta L \approx -0.2257 \epsilon \Delta (1 - \Delta^2) \frac{y}{L}$$

which turns out to be less than 2 percent for the examples computed herein.

REFERENCES

1. Goldstein, Richard J.: Film Cooling. In *Advances in Heat Transfer*, Vol. 7, Thomas F. Irvine, Jr., and James P. Hartnett, eds., Academic Press (London), 1971, pp. 321-379.
2. Seban, R. A.; and Back, L. H.: Effectiveness and Heat Transfer for a Turbulent Boundary Layer with Tangential Injection and Variable Free-Stream Velocity. *Jour. Heat Transfer*, Vol. 84, No. 3, Aug. 1962, pp. 235-244.
3. Stollery, J. L.; and El-Ehwany, A. A. M.: A Note on the Use of a Boundary-Layer Model for Correlating Film-Cooling Data. *Int. Jour. Heat Mass Transfer*, Vol. 8, No. 1, Jan. 1965, pp. 55-56.
4. Hatch, James E.; and Papell, Stephen S.: Use of a Theoretical Flow Model to Correlate Data for Film Cooling or Heating an Adiabatic Wall by Tangential Injection of Gases of Different Fluid Properties. NASA TN D-130, 1959.
5. Pai, B. R.; and Whitelaw, J. H.: The Prediction of Wall Temperature in the Presence of Film Cooling. *Int. Jour. Heat Mass Transfer*, Vol. 14, No. 3, Mar. 1971, pp. 409-426.
6. Seban, R. A.; and Back, L. H.: Velocity and Temperature Profiles in Turbulent Boundary Layers with Tangential Injection. *Jour. Heat Transfer*, Vol. 84, No. 1, Feb. 1962, pp. 45-54.
7. Nicoll, W. B.; and Whitelaw, J. H.: The Effectiveness of the Uniform Density, Two-Dimensional Wall Jet. *Int. Jour. Heat Mass Transfer*, Vol. 10, No. 5, May 1967, pp. 623-639.
8. Goldstein, Marvin E.; and Braun, Willis: Injection of an Attached Inviscid Jet at an Oblique Angle to a Moving Stream. NASA TN D-5501, 1969.
9. Braun, Willis; and Goldstein, Marvin E.: Analysis of the Mixing Region for a Two-Dimensional Jet Injected at an Angle to a Moving Stream. NASA TN D-5531, 1969.
10. Samuel, A. E.; and Joubert, P. N.: Film Cooling of an Adiabatic Flat Plate in Zero Pressure Gradient in the Presence of a Hot Mainstream and Cold Tangential Secondary Injection. *Jour. Heat Transfer*, Vol. 87, No. 3, Aug. 1965, pp. 409-418.
11. Kacker, S. C.; and Whitelaw, J. H.: The Effect of Slot Height and Slot Turbulence Intensity on the Effectiveness of the Uniform Density, Two-Dimensional Wall Jet. *Jour. Heat Transfer*, Vol. 90, No. 4, Nov. 1968, pp. 469-475.
12. Garner, H. C.: The Development of Turbulent Boundary Layers. R. & M. 2133, British ARC, June, 1944.

13. Millis, R.D. : Numerical and Experimental Investigations of the Shear Layer Between two Parallel Streams. *Jour. Fluid Mech.*, Vol. 33, pt.3, Sept. 2, 1968, pp. 591-616.
14. Goldstein, Sydney: On Backward Boundary Layers and Flow in Converging Passages. *Jour. Fluid Mech.*, Vol. 21, pt. 1, 1965, pp. 33-45.
15. Ackerberg, Robert C. ; and Glatt, Leslie: On an Integral Method for Backward Boundary Layers, *ZAMP*, Vol. 19, No. 6, Nov. 1968, pp. 882-897.
16. Burns, W.K. ; and Stollery, J.K. : The Influence of Foreign Gas Injection and Slot Geometry on Film Cooling Effectiveness. *Int. Jour. Heat Mass Transfer*, Vol. 12, No. 8, Aug. 1969, pp. 935-951.
17. Kacker, S.C. ; and Whitelaw, J.H. : An Experimental Investigation of the Influence of Slot-Lip-Thickness on the Impervious-Wall Effectiveness of the Uniform-Density, Two-Dimensional Wall Jet. *Int. Jour. Heat Mass Transfer*, Vol. 12, No. 9, Sept. 1969, pp. 1196-1201.
18. Whitelaw, James H. : An Experimental Investigation of the Two-Dimensional Wall Jet. C. P. 942, British ARC, Apr. 1966.

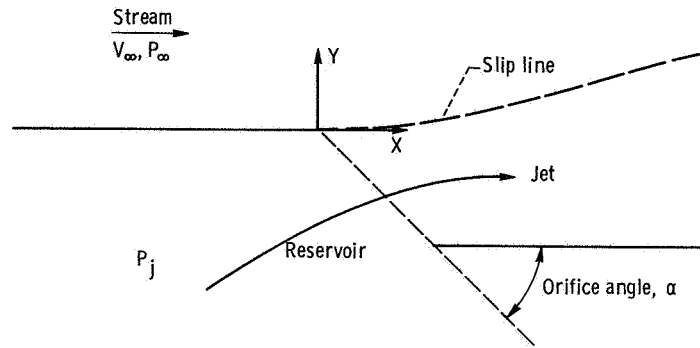


Figure 1. - Inviscid jet flow.

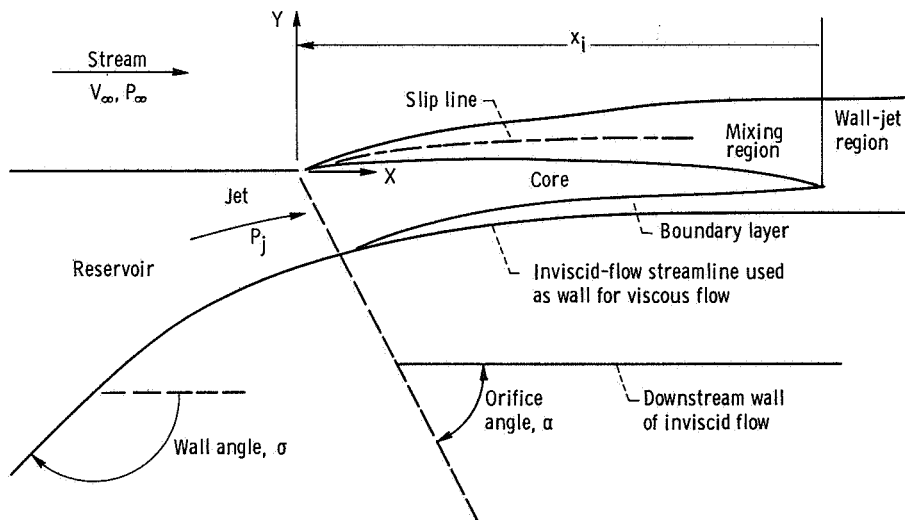


Figure 2. - Injection of jet into stream.

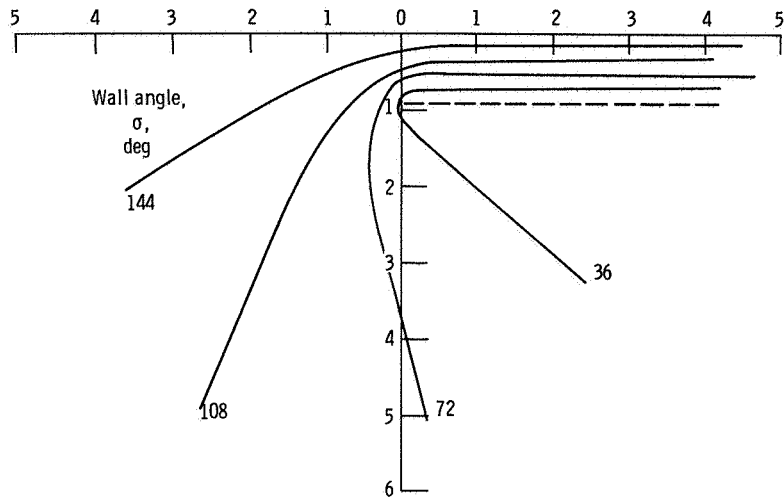


Figure 3. - Family of backward-facing steps generated by streamlines of an inviscid jet. Parameter related to orifice angle, Δ , 0.09. Coordinates in units of asymptotic width of inviscid jet, H_0 .

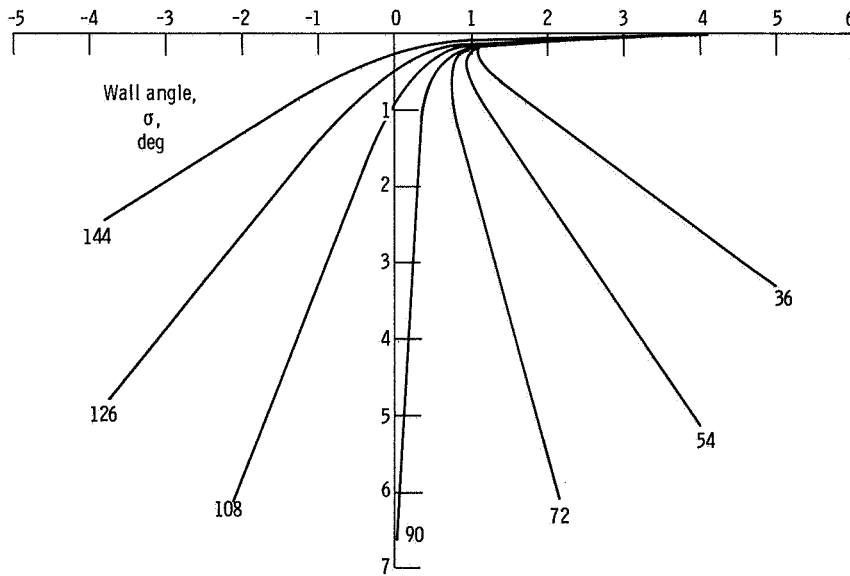


Figure 4. - Family of wall slots generated by streamlines of an inviscid jet. Coordinates in units of asymptotic width of inviscid jet, H_0 .

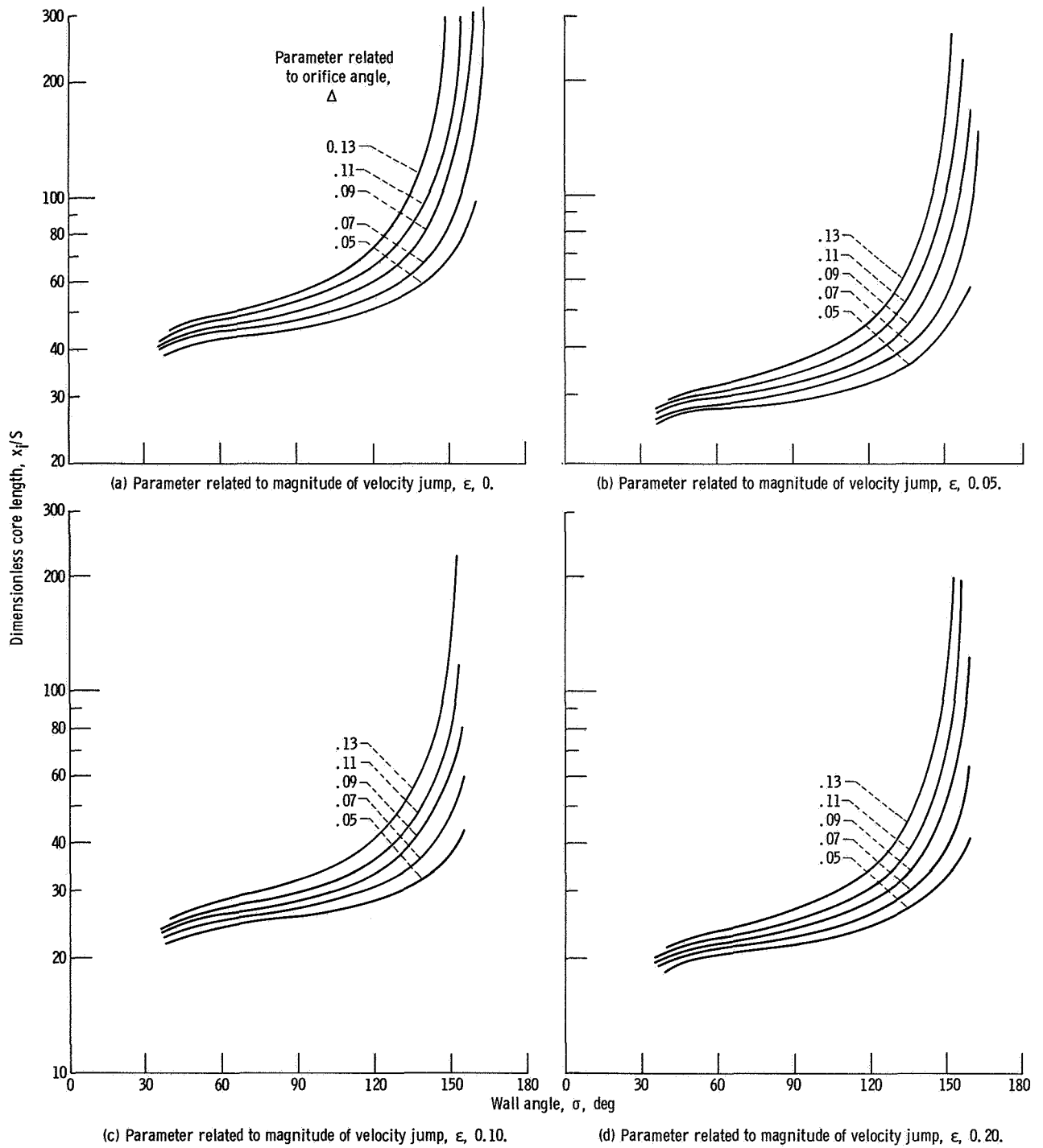


Figure 5. - Length of protective core issuing from a backward-facing step - for a Reynolds number based on step height Re_S of 10 000.

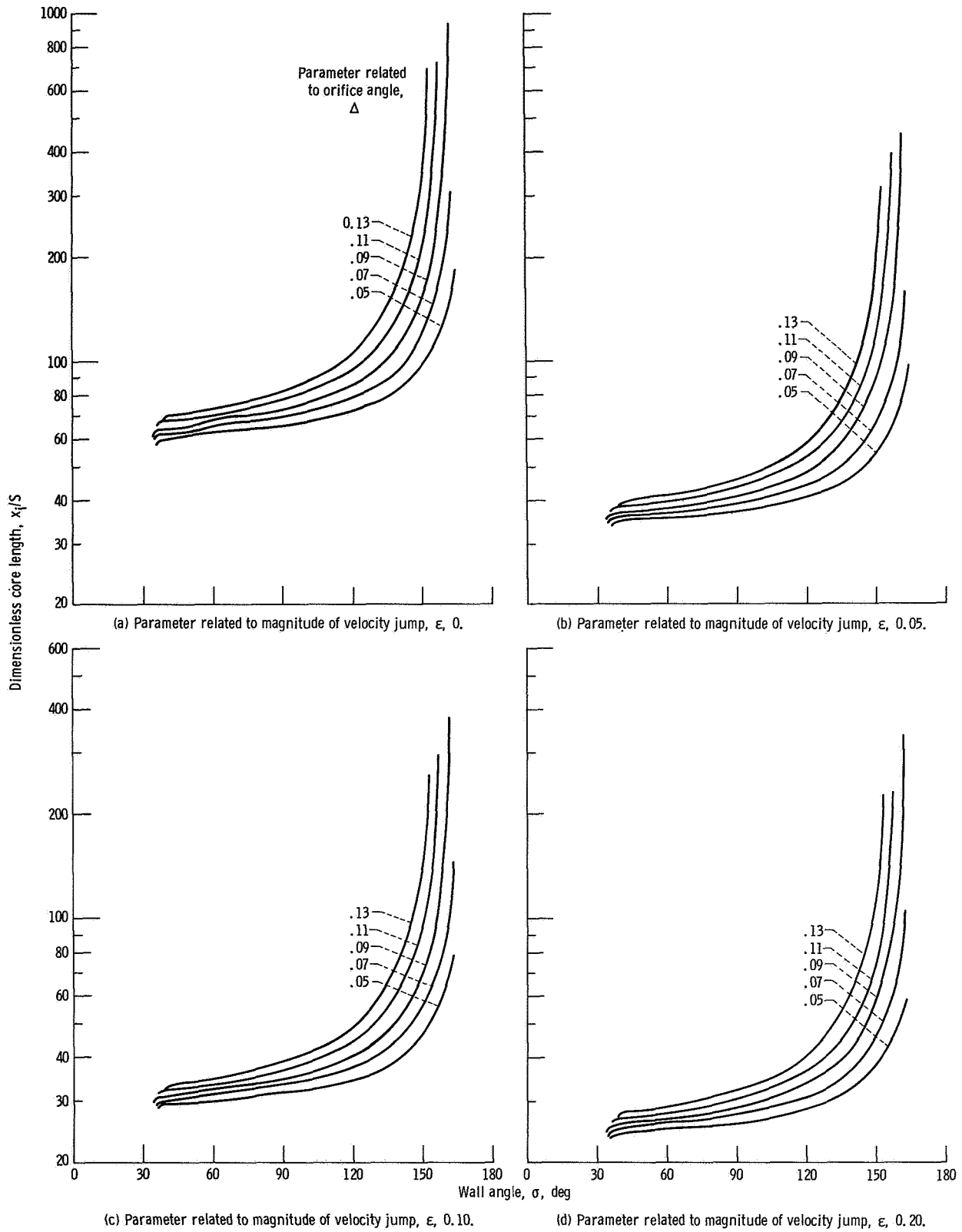
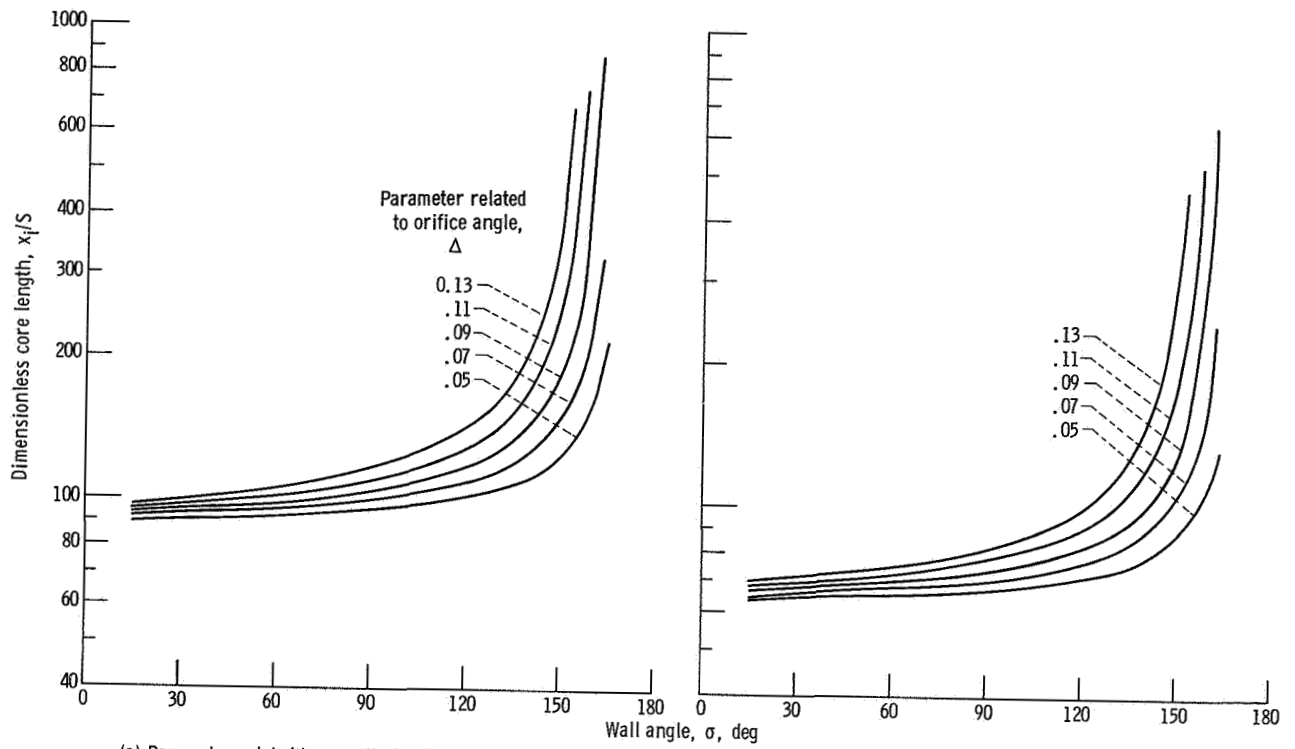
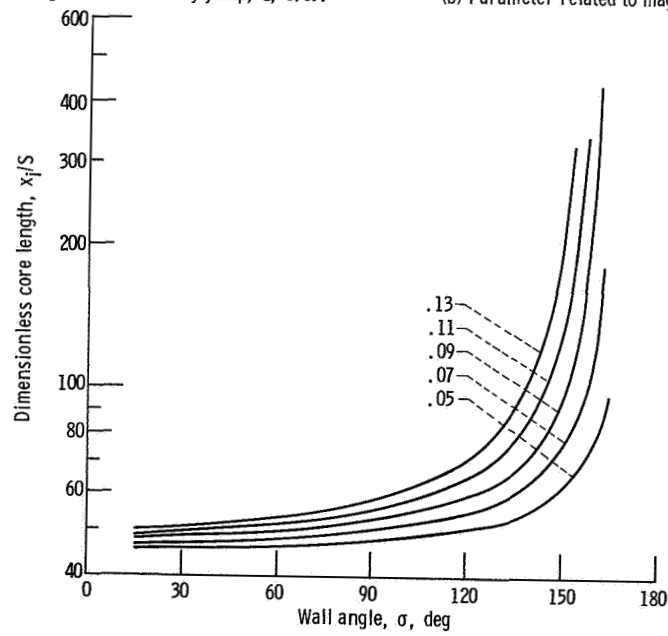


Figure 6. - Length of protective core issuing from a backward-facing step - for a Reynolds number based on step height Re_S of 100 000.



(a) Parameter related to magnitude of velocity jump, ϵ , 0.05.

(b) Parameter related to magnitude of velocity jump, ϵ , 0.10.



(c) Parameter related to magnitude of velocity jump, ϵ , 0.20.

Figure 7. - Length of protective core issuing from a backward-facing step - for a Reynolds number based on step height Re_S of ∞ .

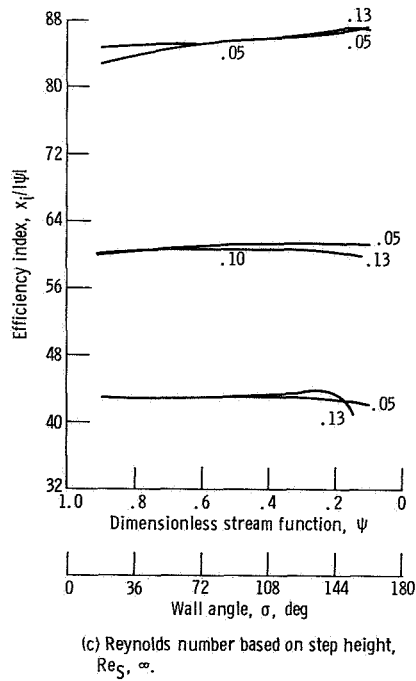
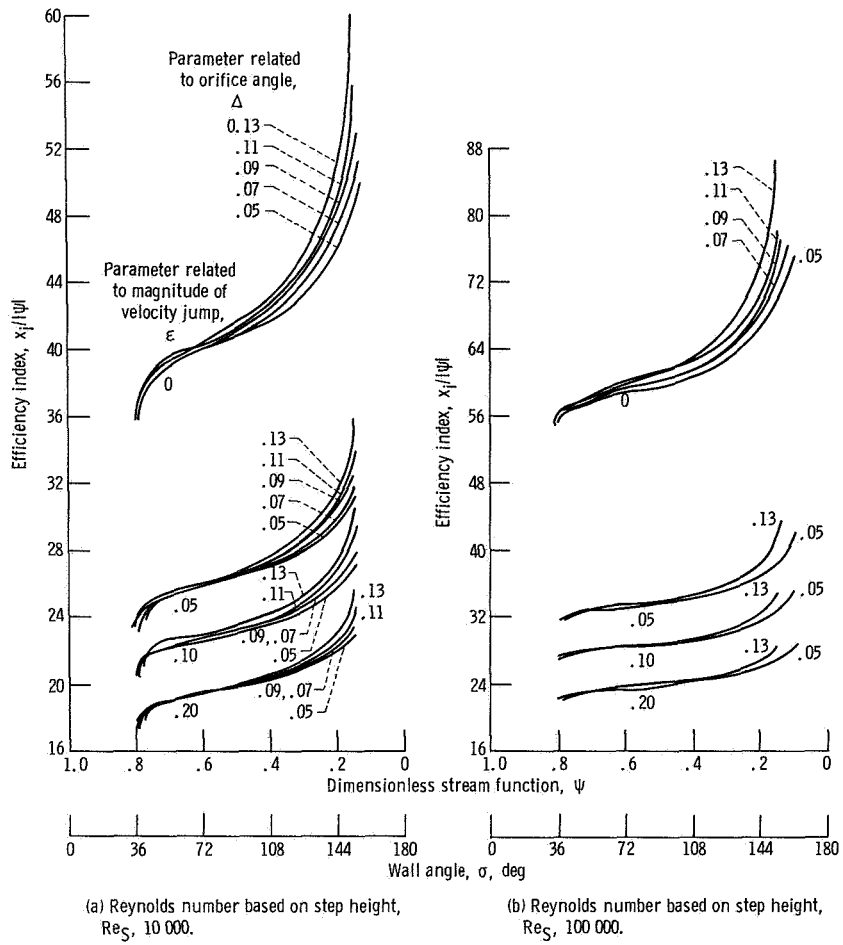


Figure 8. - Efficiency index for a backward-facing step.

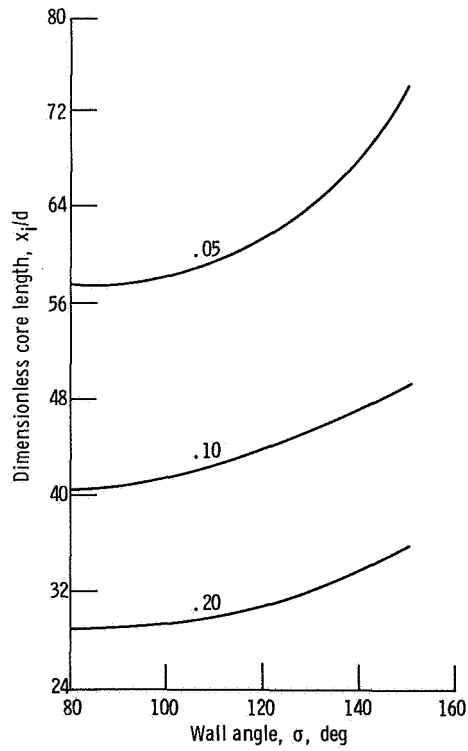
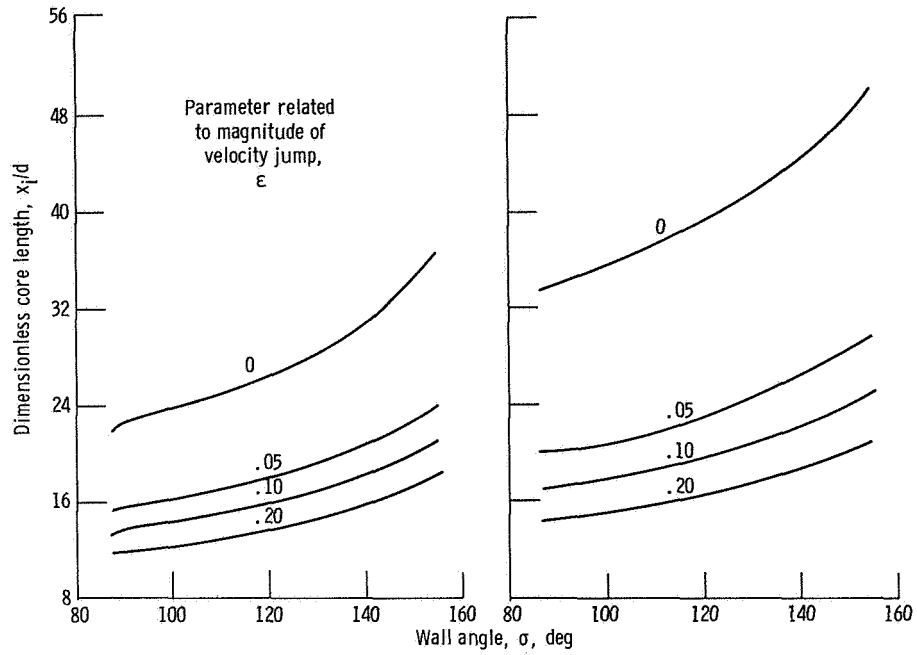
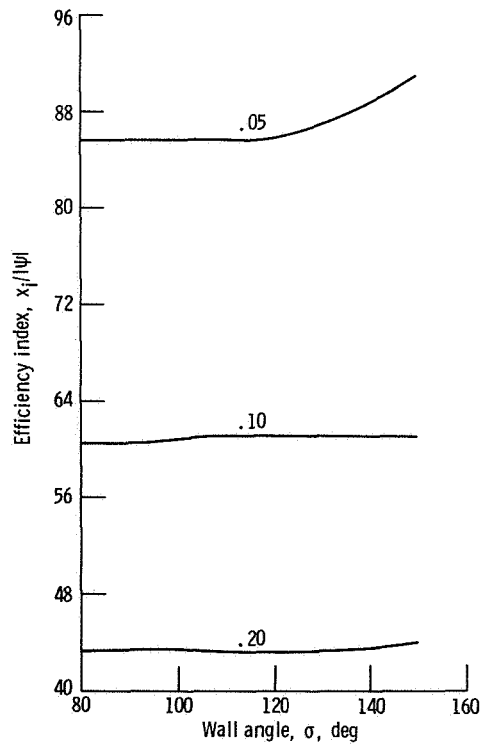
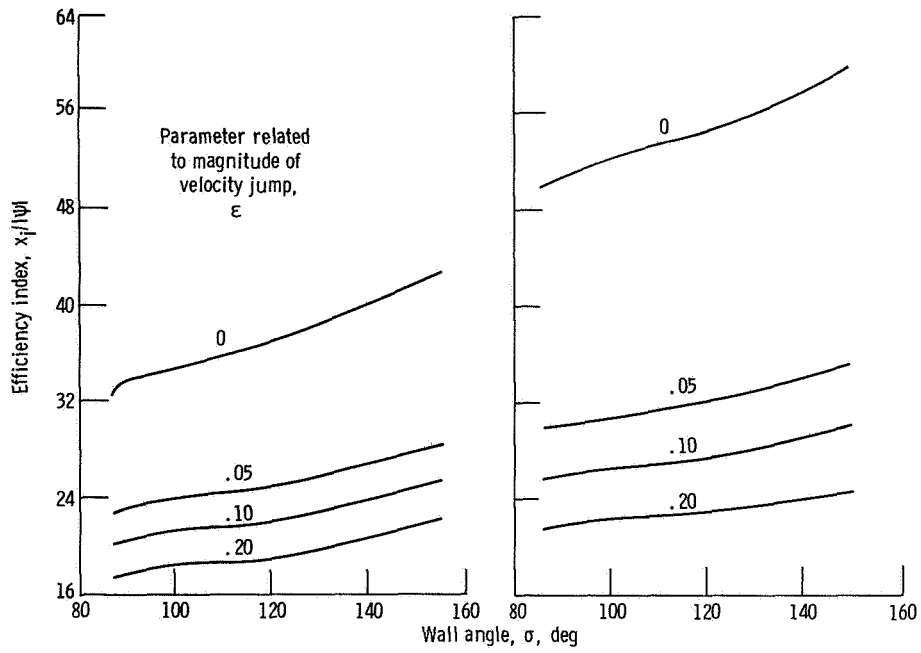


Figure 9. - Length of protective core issuing from a wall slot.



(c) Reynolds number based on slot width, Re_d, ∞ .

Figure 10. - Efficiency index for a wall slot.

NATIONAL AERONAUTICS AND SPACE ADMINISTRATION
WASHINGTON, D.C. 20546

OFFICIAL BUSINESS
PENALTY FOR PRIVATE USE \$300

**SPECIAL FOURTH-CLASS RATE
BOOK**

POSTAGE AND FEES PAID
NATIONAL AERONAUTICS AND
SPACE ADMINISTRATION
451



POSTMASTER: If Undeliverable (Section 158
Postal Manual) Do Not Return

"The aeronautical and space activities of the United States shall be conducted so as to contribute . . . to the expansion of human knowledge of phenomena in the atmosphere and space. The Administration shall provide for the widest practicable and appropriate dissemination of information concerning its activities and the results thereof."

—NATIONAL AERONAUTICS AND SPACE ACT OF 1958

NASA SCIENTIFIC AND TECHNICAL PUBLICATIONS

TECHNICAL REPORTS: Scientific and technical information considered important, complete, and a lasting contribution to existing knowledge.

TECHNICAL NOTES: Information less broad in scope but nevertheless of importance as a contribution to existing knowledge.

TECHNICAL MEMORANDUMS: Information receiving limited distribution because of preliminary data, security classification, or other reasons. Also includes conference proceedings with either limited or unlimited distribution.

CONTRACTOR REPORTS: Scientific and technical information generated under a NASA contract or grant and considered an important contribution to existing knowledge.

TECHNICAL TRANSLATIONS: Information published in a foreign language considered to merit NASA distribution in English.

SPECIAL PUBLICATIONS: Information derived from or of value to NASA activities. Publications include final reports of major projects, monographs, data compilations, handbooks, sourcebooks, and special bibliographies.

TECHNOLOGY UTILIZATION PUBLICATIONS: Information on technology used by NASA that may be of particular interest in commercial and other non-aerospace applications. Publications include Tech Briefs, Technology Utilization Reports and Technology Surveys.

Details on the availability of these publications may be obtained from:

SCIENTIFIC AND TECHNICAL INFORMATION OFFICE

NATIONAL AERONAUTICS AND SPACE ADMINISTRATION

Washington, D.C. 20546